

VIBROSEIS* IN THE CANADIAN ARCTIC — A CASE STUDY

DAVID BIRNIE¹ and FRED EASTWOOD¹

ABSTRACT

From February to May 1980, Chevron Standard Limited conducted a 1 200% VIBROSEIS program on Northeast Banks Island — the first time Chevron standard has operated a VIBROSEIS crew in the Canadian Arctic. In this remote and difficult operating environment, VIBROSEIS was chosen for the following reasons:

1. It was more environmentally acceptable.
2. It would result in a lower over-all cost per kilometre than would dynamite data.
3. With VIBROSEIS the system could be easily designed or "engineered" to get rid of a troublesome surface wave generated at the air-permafrost interface with an apparent horizontal velocity of approximately 1 650 m/s.
4. It was felt that VIBROSEIS would not generate permafrost or "ice" breaks, which are characteristic of dynamite data in the arctic.

A noise analysis was conducted which resulted in the following significant parameters: 40 m group length, 120 m drag and a 65-20 Hz sweep. With these parameters, almost all the surface wave energy was attenuated. The quality of the resulting production data is superior to that of dynamite data previously obtained in the same area.

A detailed analysis of the data obtained provides some useful insight into, as well as a review of, how the VIBROSEIS method works.

INTRODUCTION

From February to May 1980, Chevron Standard Limited conducted a 1 200% VIBROSEIS program on Northeast Banks Island in the high arctic. Grant Geophysical was the contractor and provided the men and equipment. The study area is outlined in Figure 1, and is at a latitude of roughly 74° north and a longitude of 177° west. It cannot be overemphasized that the difficult operating conditions are the overriding consideration in the design of any field program in this type of environment. Figure 2 illustrates typical weather conditions expected for this part of the world.

The advance crew started moving equipment into the project area 1981-01-21, in 24 hours of darkness. The operation was completed 1981-05-10,

in 24 hours of daylight. The exploration objectives have to be accomplished within this four-month operational window. With this type of high-cost program, it becomes especially important to optimize both data quantity and data quality.

BACKGROUND

In order to aid in our understanding of the type of problem to expect, well before the start-up of field operations we conducted a literature search and, in addition, analyzed some nearby existing dynamite data. Figure 3 is an illustration from a paper by Bob Merritt entitled, "Seismic Reflection Measurements in the Canadian Arctic Islands," and provided us with some useful background material. Illustrated are several profiles taken from various areas in the Arctic Islands. The green colouring identi-

¹Chevron Standard Limited, 500 - 5th Avenue S.W., Calgary, Alberta

The authors wish to express their appreciation to Chevron Standard Limited for permission to publish the material presented in this paper.

* Registered trade and service mark of Continental Oil Company.

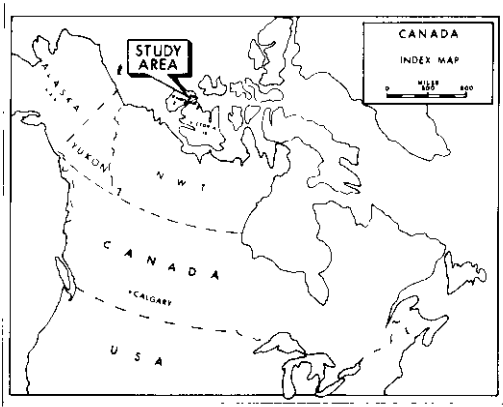


Fig. 1. Index map of study area.

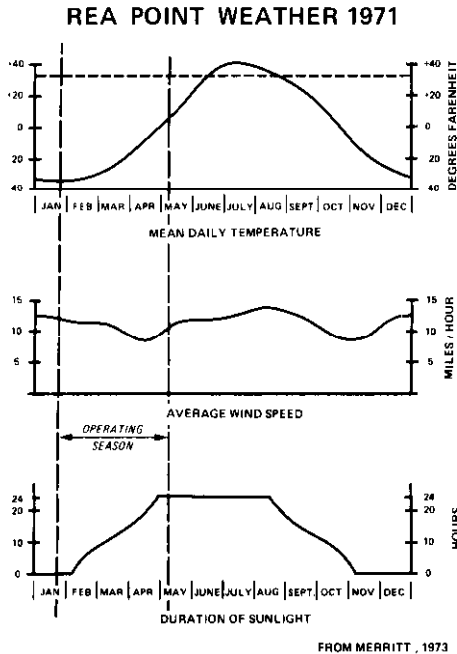
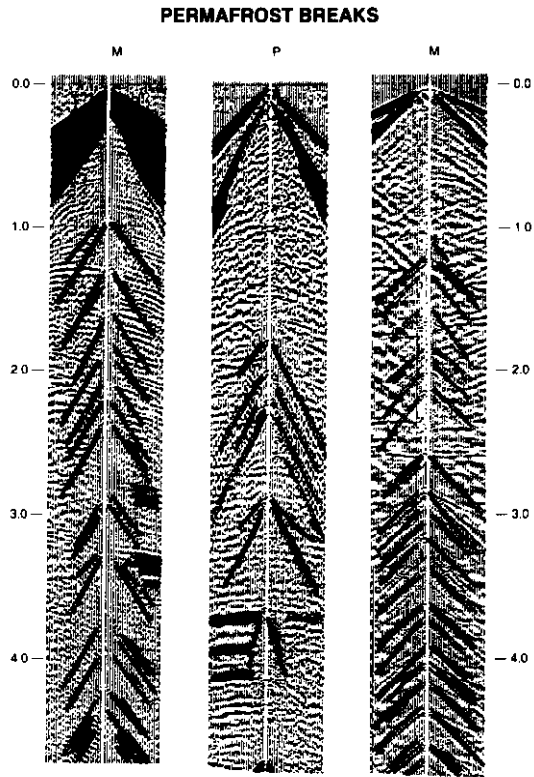


Fig. 2. Typical Arctic weather conditions.

fies the first-break energy, and the blue identifies the reflection energy. Shaded in red is a surface wave with a velocity of roughly 1 500 m/s to 1 800 m/s (5 000 ft/s to 6 000 ft/s). This wave has many of the characteristics of a Rayleigh wave generated at the air-permafrost interface. The yellow shading highlights a series of permafrost or ice breaks which are characteris-



FROM MERRITT, 1973

Fig. 3. Several typical dynamite profiles from the Canadian Arctic Islands.

tic of dynamite land data in the Arctic. They vary in intensity and occur at random times after the initial blast. It is felt that ice breaks are caused by the relaxation of stresses within the permafrost layer after the initial blast.

DYNAMITE DATA

Two typical dynamite profiles from the study area are shown in Figure 4. They are plotted with no grain adjustment except for trace-to-trace equalization. Many of the features present on the profiles in Figure 3 are also present on these two profiles. A bad ice-break problem plagues the left-hand profile, and a very strong surface wave is present on both. These two profiles have been analyzed in more detail in the frequency wave number or F-K domain. Figure 5 illustrates the format Chevron uses for F-K plots.

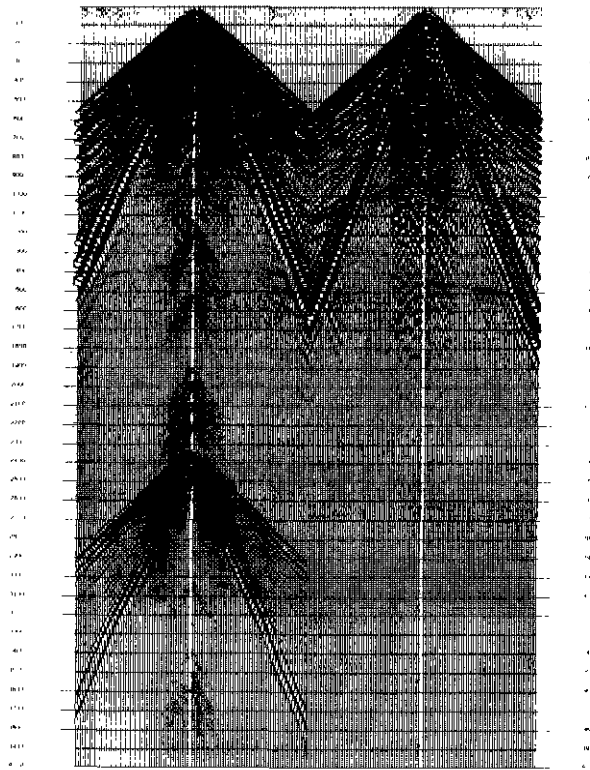


Fig. 4 Two dynamite profiles from the study area.

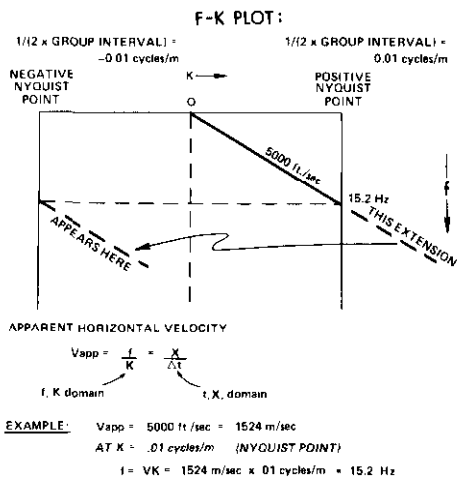


Fig. 5. Frequency wavenumber (F-K) plot format.

Figure 6 contains an F-K plot of the first 48 traces of our familiar dynamite profile. This profile has had no gain, filters or mutes applied. The events are identified by using the same colour scheme as in Figure 3. The first-break energy (shaded green) has an apparent horizontal velocity of roughly 3 800 m/s (12 500 ft/s). The Rayleigh-type surface wave (shaded red) has an apparent horizontal velocity of 1 500 m/s (5 000 ft/s). From this illustration, it becomes apparent that the amplitude of the surface wave is twice as large as that of the first breaks and roughly twenty times greater than that of the reflection energy. In addition, the surface-wave energy is broadband and ranges up to 25 Hz in this example. Clearly, simple bandpass filtering will not remove the surface-wave energy entirely (without sacrificing a significant portion of the reflection energy).

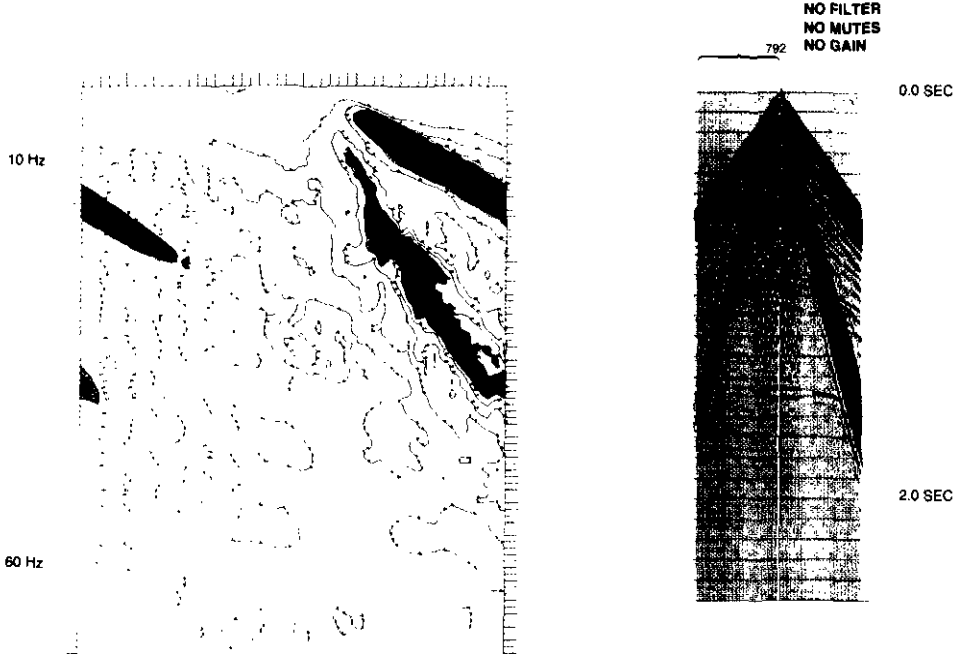
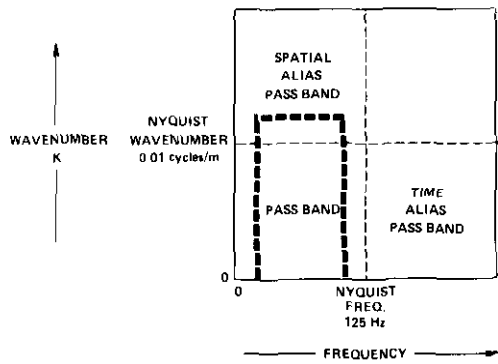


Fig. 6. F-K plot of typical dynamite profile, with no gain adjustment.



EXAMPLE. 1977 DYNAMITE DATA

$$\text{NYQUIST FREQ.} = \frac{1}{2t_n} = \frac{1}{2(0.004 \text{ sec.})} = 125 \text{ Hz}$$

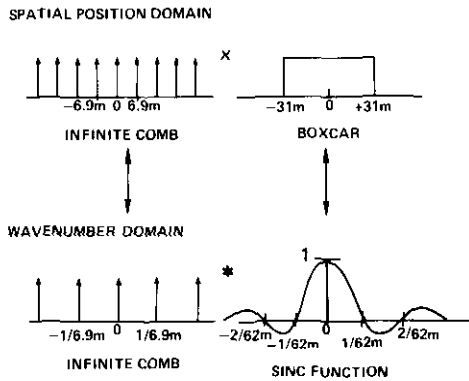
$$\text{NYQUIST WAVENUMBER} = \frac{1}{2(G.I.)} = \frac{1}{2(50\text{m})} = 0.01 \text{ cycles/m}$$

t_n = sampling rate
G.I. = group interval

Fig. 7. Typical seismic energy pass band, in the frequency-wavenumber domain.

1977 DYNAMITE DATA

- (1) POINT SOURCE
- (2) RECEIVER ARRAY: 9 PHONE GEOPHONE GROUP SPREAD OVER 55m



THIS ARRAY PASSES ALL WAVENUMBERS LESS THAN $1/62$ cycles/m FOR A SURFACE WAVE WHICH TRAVELS AT 5000 ft./sec. = 1524m/sec.

$$f = vK = 1524 \times 1/62 = 24.6 \text{ cycles/sec.}$$

Fig. 8. Array filter for 1977 dynamite data.

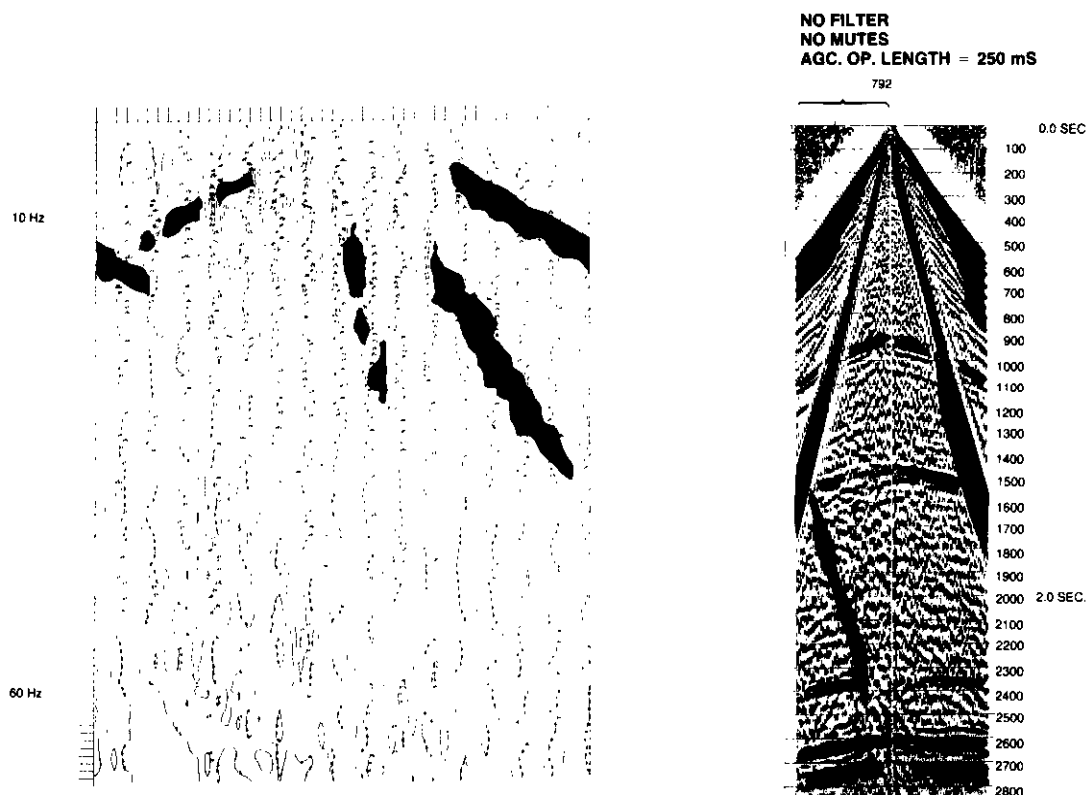


Fig. 9. F-K plot of dynamite profile, after AGC gain adjustment.

In the seismic industry, recording is normally restricted to within a nonaliased frequency pass band. That is, we try not to record any energy beyond the Nyquist frequency by selecting appropriate sampling rates and field filters. However, in the wave number or K domain, spatially aliased energy is often recorded. This is because group intervals and group lengths, which affect the Nyquist Point and array filter, are more often dictated by other operating considerations (such as avoiding overlapping groups, etc.). In any event, spatially aliased energy does not become a severe problem until it wraps around back into the reflection energy, which is near the $K = 0$ axis.

The dashed box in Figure 7 diagrammatically illustrates the energy pass band for typical seismic surveys. It is clearly visible in Figure 6 that some of the surface-wave energy (shaded red) is spatially aliased.

The abrupt termination of the aliased surface-wave energy is a function of the array para-

meters used for this survey. These 1977 dynamite data were recorded by using single shots and nine geophones spread over 55 m. Figure 8 illustrates how these parameters are represented mathematically. In the wave-number domain, the array filter is a SINC function (*i.e.*, SINX/X) with its first zero crossing at $1/62$ m. This theoretical cutoff matches exactly with the observed termination of the aliased surface-wave energy.

It is illustrative to follow a simplified process flow scheme and observe the effects on the various energy forms. The first step is to apply AGC gain to balance the energy down the section, as in Figure 9. The reflection energy (in blue) is now identifiable, also evident is back-scattered energy (shaded orange). Following the gain adjustment, the first-break and surface-wave energy is muted out, as shown in Figure 10. These mutes seriously reduce coverage on the shallow events of interest and, at times, the nominal coverage of 600% is halved. Finally, a bandpass filter is applied to enhance the reflec-

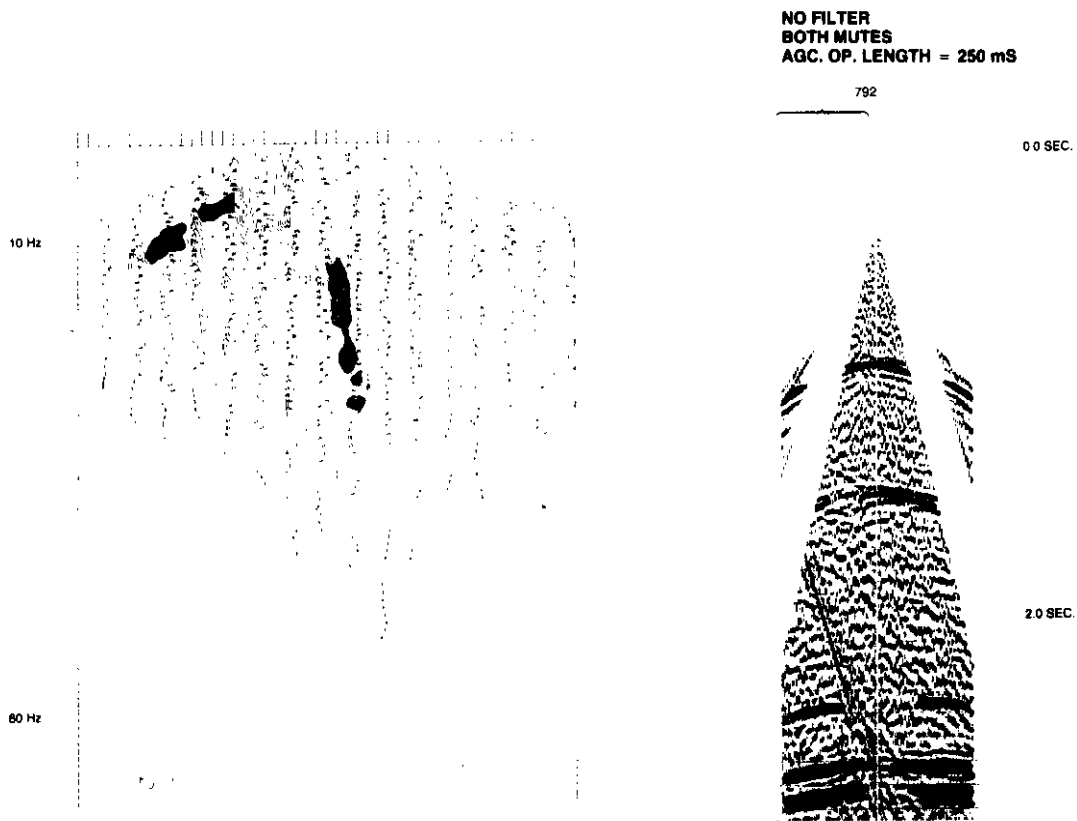


Fig. 10. F-K plot of dynamite profile, after muting of first-break and surface-wave energy.

tion energy, as in Figure 11. The reflection energy has now been considerably enhanced as compared with Figure 6. This profile is now ready to have statics and normal moveout applied, then be stacked with others to produce the final stacked section.

Figures 12 and 13 give us a comparison between the two dynamite profiles from Figure 4. Both profiles have had the same spherical-divergence gain function applied. The ice breaks in Figure 13 persist through even a sixfold stack. The dashed vertical line in Figure 13 represents the first zero crossover in the wave-number domain due to the geophone array, and any aliased ice-break/surface-wave energy (in red)

appearing to the right of this line is side-lobe energy. Notice that the surface-wave energy pattern mirrors the theoretical-array attenuation function (the SINC function) that we determined earlier in Figure 8. This side-lobe energy interferes with the reflection energy at approximately 40 Hz, and has negative consequences if we try to use a velocity filter to remove the surface-wave and ice breaks.

Before any field testing, several areas of concern have been isolated, notably the surface wave, which reduces coverage shallow in the section, and the ice break problem, which renders many dynamite profiles virtually useless.

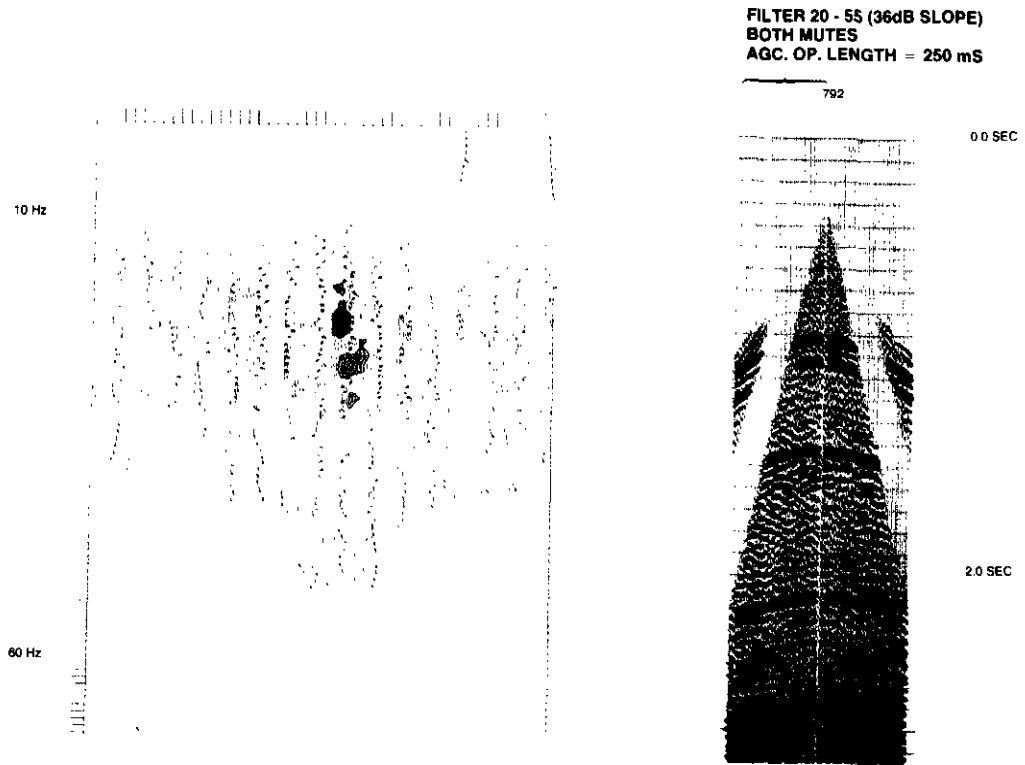


Fig. 11. F-K plot of dynamite profile, after bandpass filtering.

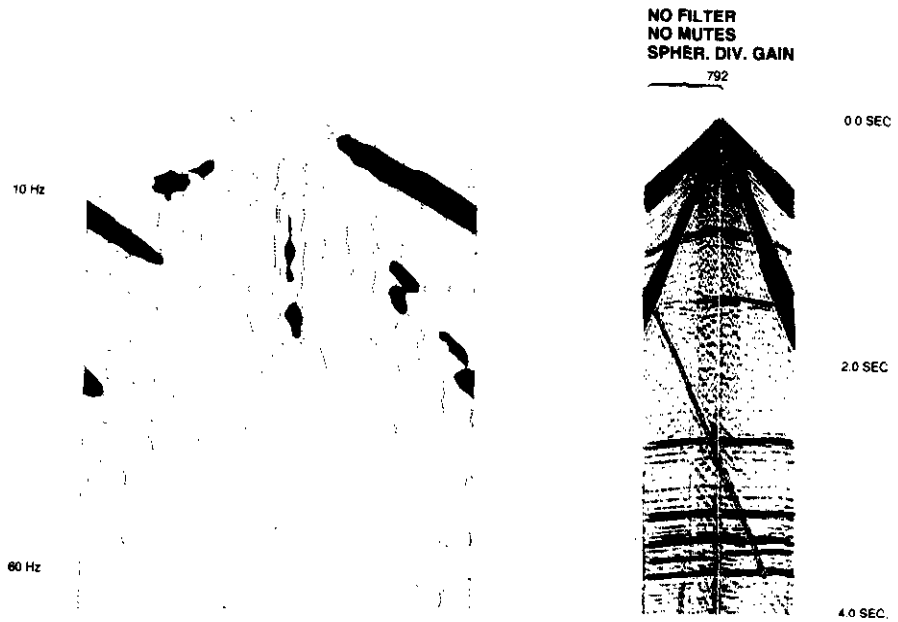


Fig. 12. F-K plot of dynamite profile, after spherical-divergence gain adjustment.

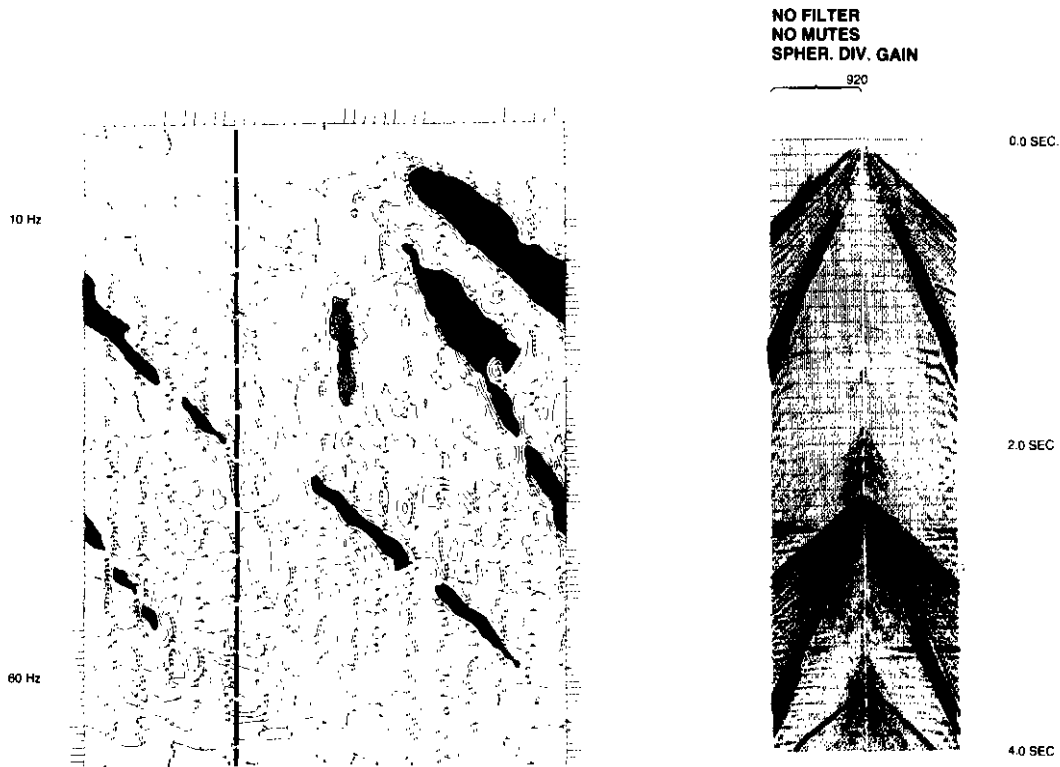


Fig. 13. F-K plot of dynamite profile, with ice breaks, after spherical-divergence gain adjustment.

NOISE TEST

To aid in our understanding of these noise problems, during the first day of field recording we performed a VIBROSEIS walk-away noise analysis. The spread geometry is illustrated in Figure 14 and explained in Table 1. The geophone spread consisted of six traces, 5 m apart. Each trace consisted of nine geophones bunched together to simulate a point receiver. The four vibrators were positioned side by side to simulate a point source. They moved progressively away from the geophone spread, vibrating in a particular fashion at each of the six composite locations A through F. This procedure yields a series of profiles ranging in offset from 5 m to 3 000 m. Figure 15 illustrates how each composite is made up in detail. Each record is defined as the four vibrators sweeping simultaneously once only. This particular combination of records was chosen so that in the processing centre, a variety of source arrays could be simulated.

Examples of some individual records from composite A, before cross correlation, are shown

in Figure 16. No gain or trace-to-trace equalization has been applied. The four vibrators swept down from 80 Hz to 20 Hz over 12 seconds, and recording continued for 4 additional seconds.

Hence, the total record length is 16 s. After cross correlation, the record length is collapsed to 4 s (see Fig. 17), and it has become evident that most of the energy on these records is concentrated in the surface-wave and first breaks. Any energy visible further down the profiles is correlation noise, not reflection energy.

After completion of the walk-away procedure, the field tapes were flown back to Calgary, and different array parameters were simulated by Chevron's processing centre, using the basic processing flow outlined in Figure 18. The processing primarily involves the summing and stacking of the various 144 records in different manners, in order to simulate different source and receiver arrays. In the meantime, the crew continued with a set of interim parameters outlined in brackets in Table 2.

N.E. BANKS ISLAND VIBROSEIS WALKAWAY NOISE ANALYSIS

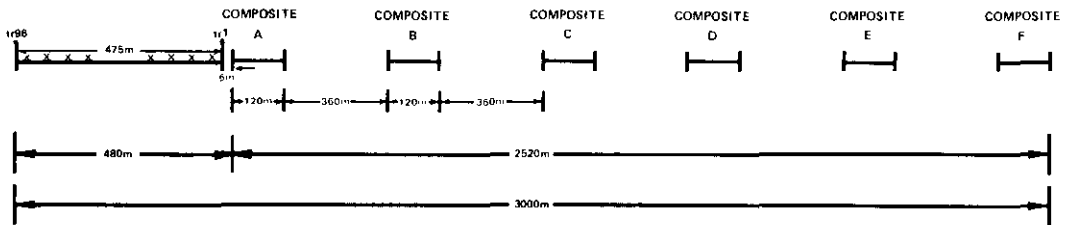


Fig. 14. Geometry of VIBROSEIS noise spread.

GEOPHONE SPREAD (SEE FIGURE 14)

- 96 TRACES
- 9 PHONES BUNCHED TOGETHER FOR EACH GROUP
- GROUP SPACING 5m
- TOTAL SPREAD LENGTH 475m

VIBRATING PROCEDURE (SEE FIGURES 14, 15)

- ON FIGURE 14 ARE SHOWN 6 IDENTICAL VIBRATING POINT COMPOSITES (A,B,C,etc.) EACH OF LENGTH 120m
- WITHIN EACH COMPOSITE ARE 13 INDIVIDUAL VIBRATING POINT LOCATIONS (NUMBERED 1 TO 13 IN FIGURE 15) 10m APART
- SHOWN IN FIGURE 15 ARE THE NUMBER OF RECORDS PRODUCED AT A PARTICULAR VIBRATING LOCATION FOR EXAMPLE IN VIBRATING LOCATION NO. 5, 3 RECORDS ARE PRODUCED
- TO PRODUCE ONE RECORD THE 4 VIBRATORS STAND SIDE BY SIDE AND SIMULTANEOUSLY SWEEP ONCE FOR 12 SECONDS (20/80 Hz) AND A 16 SECOND RECORDING IS MADE (FOR EXAMPLE AT VIBRATING LOCATION No. 5 THIS PROCEDURE IS REPEATED 3 TIMES AND 3 SEPARATE RECORDS ARE PRODUCED.)
- THERE ARE 24 RECORDS PRODUCED IN EACH COMPOSITE (144 RECORDS IN TOTAL)

Table 1. Procedure used for noise test.

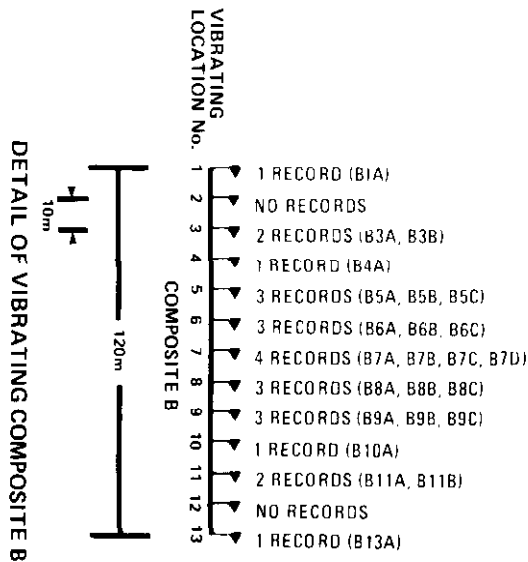


Fig. 15. Detail of vibrating composite B.

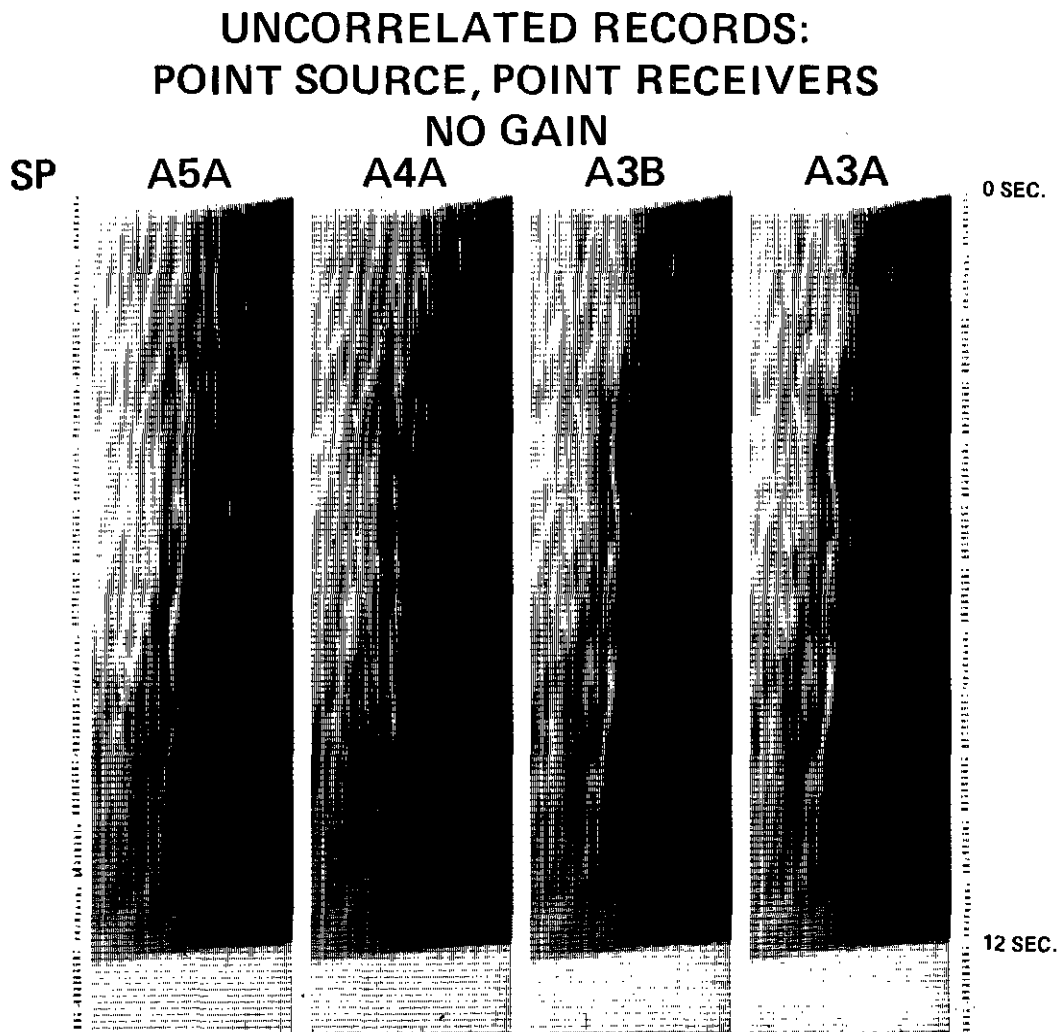


Fig. 16. Typical uncorrelated records from noise test.

The results of the field tests are summarized in Figure 19. The nine panels are the same profile with only different simulated source and receiver array lengths. As the array lengths increase, it is easy to see the progressive attenuation of the surface wave. With the longer arrays, the surface wave is difficult to identify and the reflection energy shows good continuity through this noisy zone. The final field parameters that were chosen are outlined in Table 2. It was felt that a vibrator drag of 120 m and a 40 m group length provided optimum data with minimum operating difficulties.

Now let us look at this choice of parameters from an array-filtering point of view. The 120 m drag consists of the four vibrators in line 20 m apart, sweeping 16 times, moving up 4 m between each sweep. This source array can be approximated mathematically as a triangular source of length 136 m (see Fig. 20). The combined array-filtering effect of the source and receiver array is outlined in Figure 21. In the wave-number domain, the combined array-filter function is a complex $\text{SINC}^2 \times \text{SINC}$ function. The first zero crossover is at a wave number of $1/68$ m, and the side lobes are negligibly small.

CORRELATED RECORDS: POINT SOURCE, POINT RECEIVERS NO GAIN

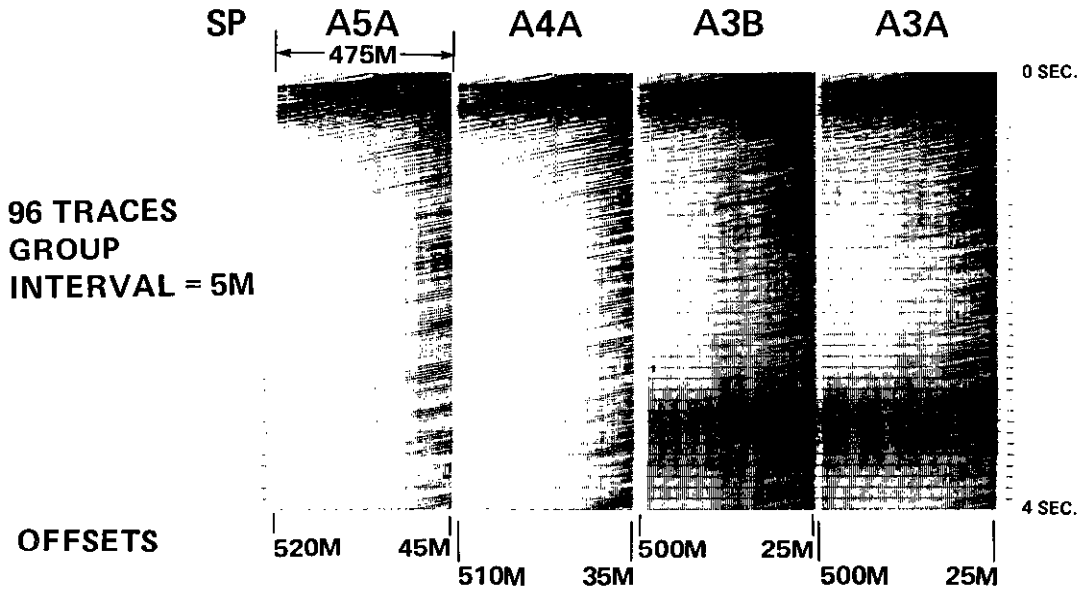


Fig. 17. Typical correlated records from noise test.

NORTHEAST BANKS ISLAND FIELD PARAMETERS

'77 DYNAMITE 600%
2414-50-* -50-2414, 96 TRACE
(7920'-165'-* -165'-7920')
9 PHONES OVER 55m (180')
GROUP INTERVAL 50m (165')
SINGLE HOLE 18 kg @ 18m (40 lb. @ 60')
SHOT POINT INTERVAL 400m (1320')
FIELD FILTERS 8 HZ/18dB/OCT.-128 HZ

'80 VIBROSEIS 1200%
2240-360-* -360-2240, 96 TRACE
9 PHONES OVER 40m
GROUP INTERVAL 40m
DRAG 120m, 4 X 16 SWEEPS, 65-20 HZ
SHOT POINT INTERVAL 160m

INTERIM PARAMETERS
1650-240-* -240-1650, 96 TRACE
18 PHONES OVER 60m
GROUP INTERVAL 30m
DRAG 90m, 4 X 16 SWEEPS, 80-20 HZ
SHOT POINT INTERVAL 120m

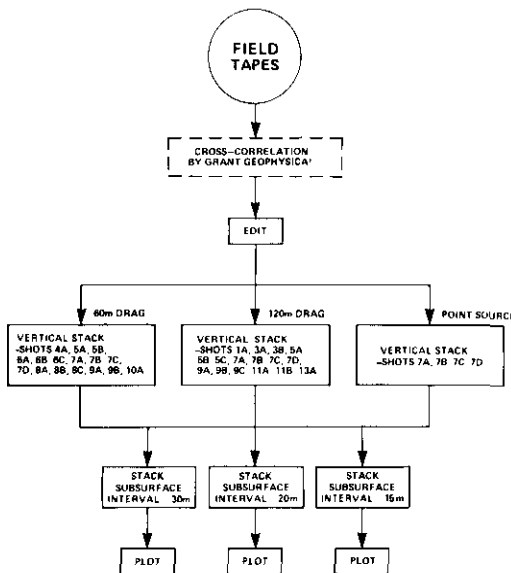


Fig. 18. Process flow for noise test.

Table 2. Field parameters used for 1977 dynamite data and 1980 VIBROSEIS Data.

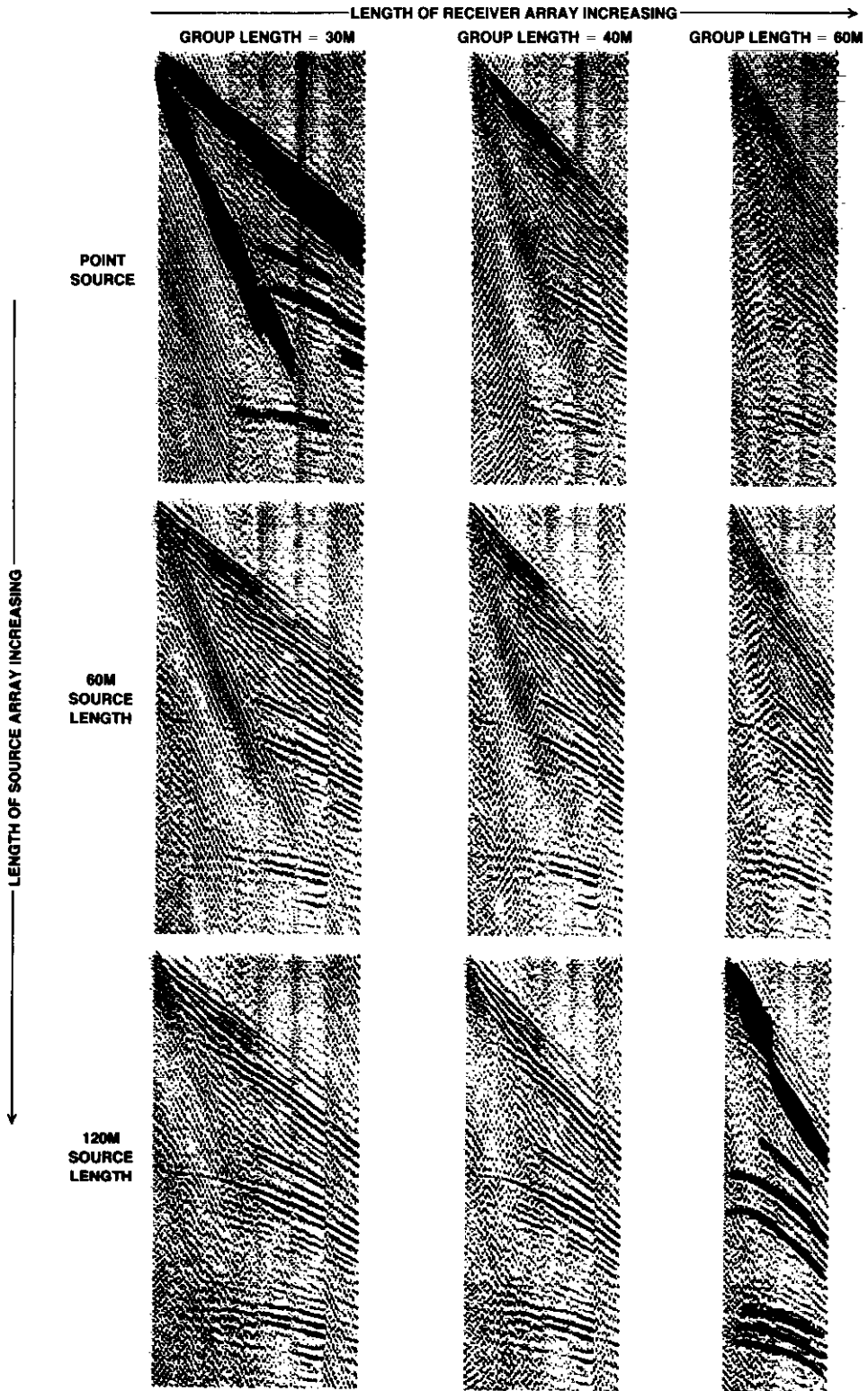


Fig. 19. VIBROSEIS noise test results.

In terms of the surface-wave energy, with an apparent horizontal velocity of 1 524 m/s (5 000 ft/s), only frequencies less than 22.4 Hz will be passed (see Table 3).

VIBROSEIS DATA

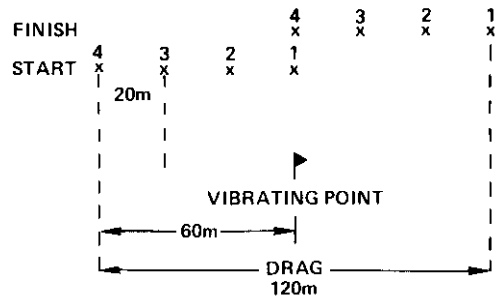
These theoretical results are confirmed by actual VIBROSEIS profiles. Figure 22 is an F-K plot of a typical such profile. The oblong pod of aliased energy, shaded red, is all that remains of the surface wave. The effect of the surface wave has been almost entirely eliminated through a combination of sweep and array design. The vertical dashed line represents the theoretical-array cutoff in the wave-number domain. The sloping dashed line represents where the surface-wave energy should plot but is absent because the VIBROSEIS sweep terminates at 20 Hz. In comparing Figures 9 and 22, the shallow events are correlatable from full offset to full offset on the VIBROSEIS data whereas, with the dynamite data, the shallow-reflection energy is completely obliterated in the region of the surface wave. The VIBROSEIS data allow a full 1 200% coverage on the shallow events of interest whereas, with the dynamite data, because of the need to mute out the surface waves, the coverage on the shallow events drops to roughly half of 600%, or 300%.

Figures 23 and 24 give a comparison between the VIBROSEIS and dynamite data in stacked form. These are wave-equation migrated time sections comparing average-quality-VIBROSEIS data with good-quality dynamite data. The VIBROSEIS data are definitely superior in the zone of interest, roughly 0.5 to 2.5 s. Deeper in the section, though, the dynamite data appear superior. If the horizontal scale of the sections is compressed, the comparison is a little clearer, as seen in Figures 25 and 26.

One alternative to muting out the surface wave on the dynamite data is to use a velocity or F-K filter in the F-K domain to attenuate the surface wave (and ice breaks).

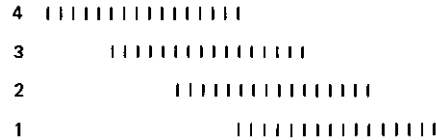
Figure 27 is an example of a dynamite section that has been velocity-filtered (before stacking) to attenuate the surface wave. The data are still inferior to the VIBROSEIS data shallow in the section; in fact, it is questionable whether velocity filtering has gained anything over conventional muting in this case.

SOURCE ARRAY



EACH VIBRATOR VIBRATES 16 TIMES OVER 60m
(MOVE UP BETWEEN SWEEPS = 4m)

VIBRATOR



31 ELEMENT SOURCE ARRAY

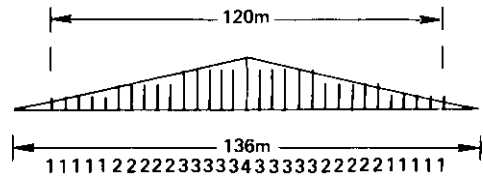


Fig. 20. 1980 VIBROSEIS source array.

EQUIVALENT ARRAY PASSES ALL WAVENUMBERS

LESS THAN 1/68 cycles/m (ALL WAVELENGTHS GREATER THAN 68m)

FREQ. \downarrow WAVELENGTH
 PHASE VELOCITY $V = f\lambda = f/K$

SUPPOSE WE HAVE A SURFACE WAVE (RAYLEIGH-TYPE) WHICH TRAVELS WITH A HORIZONTAL VELOCITY OF 5000 ft./sec. = 1524 m/sec.

$f = VK = 1524 \times 1/68 = 22.4 \text{ Hz}$

∴ ALL FREQUENCIES BELOW 22.4 Hz WILL BE PASSED.

Table 3. Effect of 1980 VIBROSEIS array filter on the surface wave.

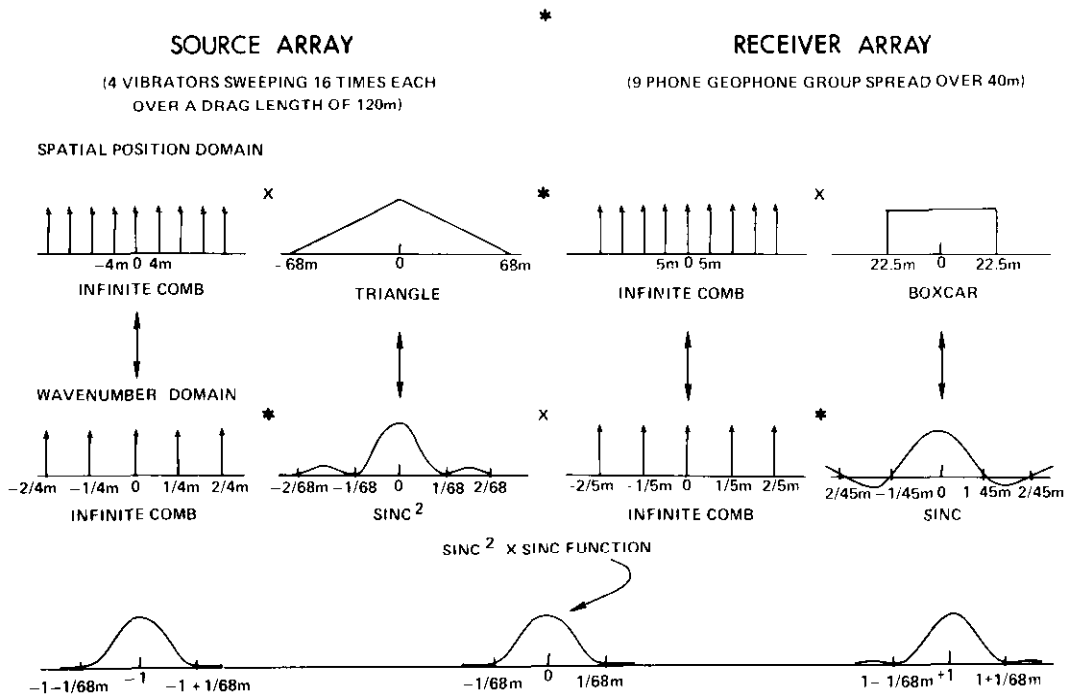


Fig. 21. Array filter for 1980 VIBROSEIS data.

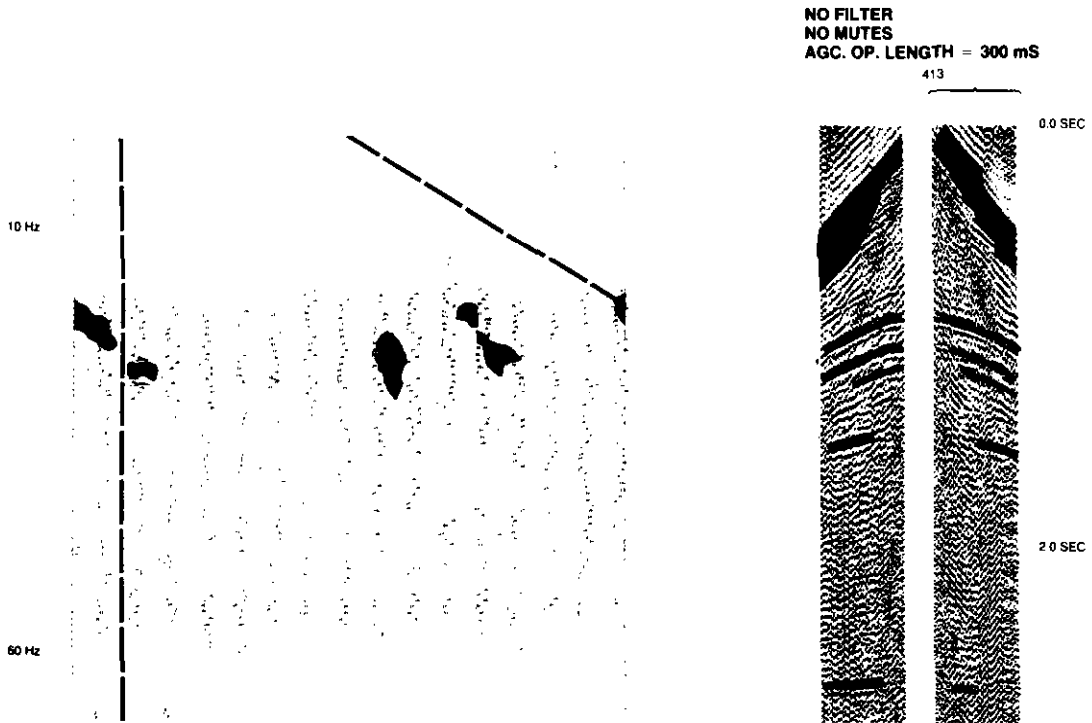


Fig. 22. F-K plot of typical VIBROSEIS profile, after AGC gain adjustment.

**1980 VIBROSEIS DATA : 1200 % MIGRATED TIME
FILTER 20-55/36 dB**

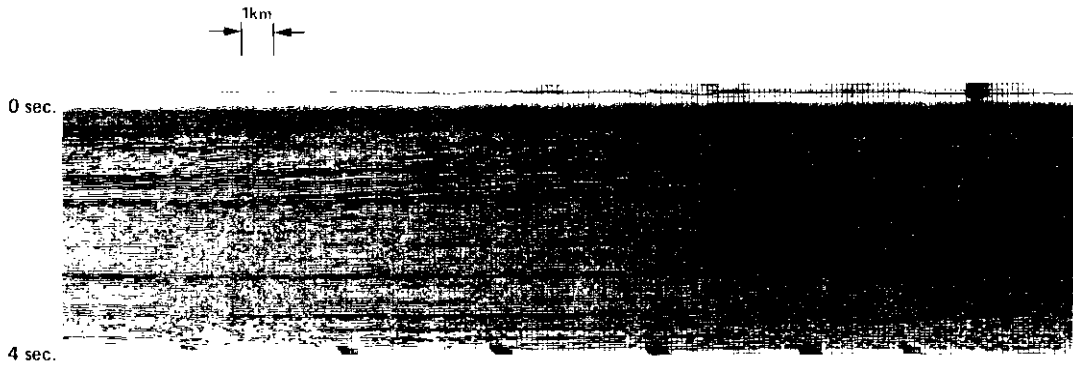


Fig. 23. 1980 VIBROSEIS data, migrated time section.

**1977 DYNAMITE DATA : 600 % MIGRATED TIME
FILTER 15-55/36 dB**

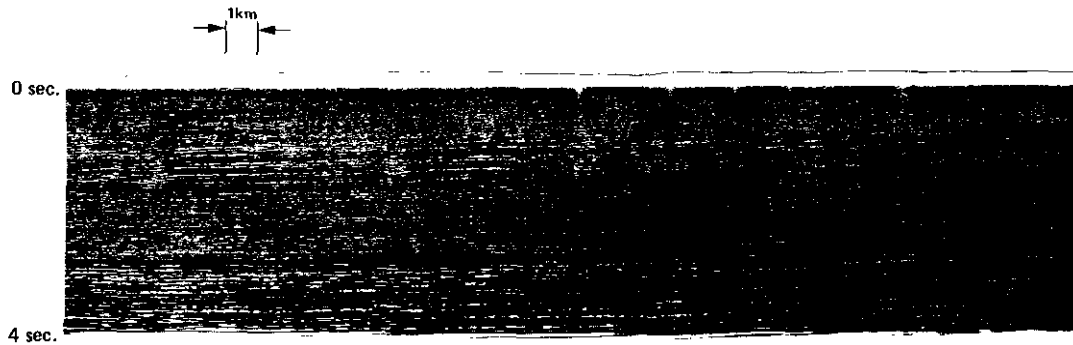


Fig. 24. 1977 dynamite data, migrated time section.

**1980 VIBROSEIS DATA: 3000% MIGRATED TIME
FILTER 20 — 55/36 dB MUTED DATA**

1 km.
→ | ←

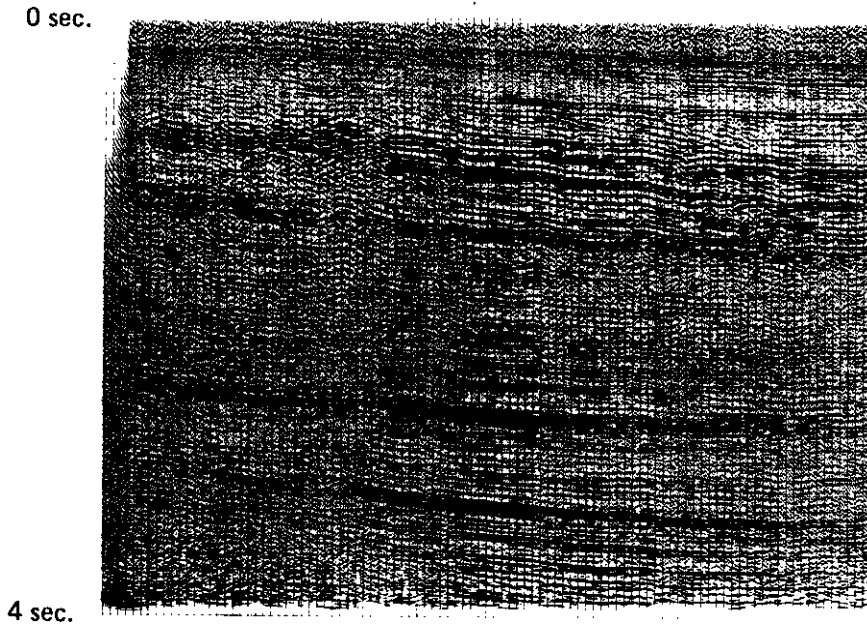


Fig. 25. 1980 VIBROSEIS data, compressed horizontal scale section.

**1977 DYNAMITE DATA: 1200% MIGRATED TIME
FILTER 5—45/24 dB FKFILTERED, NO MUTES**

1km
→ | ←

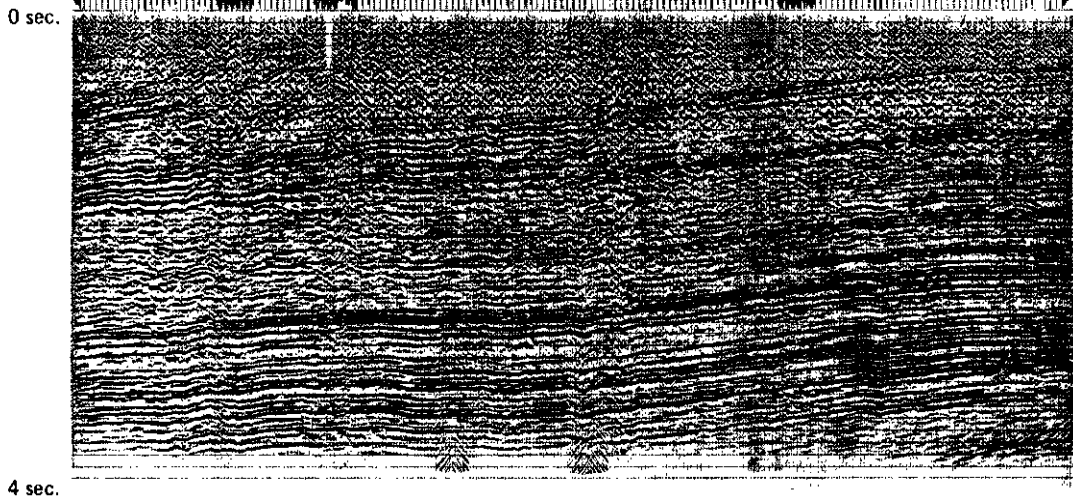


Fig. 26. 1977 dynamite data, compressed horizontal scale section.

1977 DYNAMITE DATA : 1200 % MIGRATED TIME
 FILTER 15-55/36 dB
 MUTED DATA

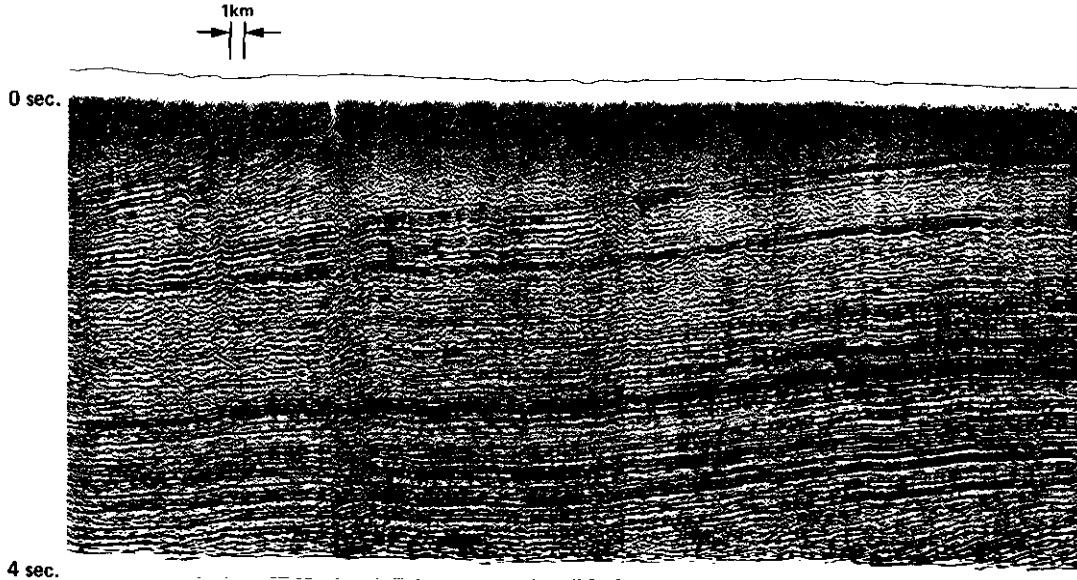


Fig. 27. 1977 dynamite data, surface wave velocity, filtered.

CONCLUSIONS

In summary, some of the advantages of the VIBROSEIS system in this situation include:

1. With VIBROSEIS no ice breaks occur.
2. Problems such as the surface wave can be overcome, because it is easier to design or engineer the parameters with VIBROSEIS than with dynamite. In Banks Island, only single shot holes were possible because of the hard frozen terrain, which eliminates the possibility of using multiple-hole patterns to help attenuate the surface wave. In addition, with VIBROSEIS the spectrum of the sweep is controllable whereas, with dynamite, there is little control over the energy spectrum of the source.
3. Along a different line, there are numerous environmental regulations in the Arctic, and any effort to minimize environmental disruption is greatly appreciated.
4. The smaller equipment and crew also have advantages when one is dealing with the logistics of moving to and from the program area.
5. Costwise, the 517 km of 1 200% vibroseis data were acquired for something over \$3 000 000. This cost compares very favourably with that

of the 460 km of 600% dynamite data acquired in 1977.

The principal disadvantage of the VIBROSEIS data is the poorer signal-to-noise ratio deeper in the section; to a lesser extent, these data were more vulnerable to wind noise. Both problems could possibly be overcome by larger vibrators and/or longer sweeps.

REFERENCES

- Al-Hussini, M. I., Barley, B. J. and Glover, J. B., Dispersion patterns of the ground roll in eastern Saudi Arabia: *Geophysics*, v. 46, no. 2.
- Cobb, A. T., 1973, "Vibroseis" applications in the Arctic: *Proceedings of the 1973 CSEG National Convention*.
- Geyer, R. L., The "Vibroseis" system of seismic mapping: *Journal of the Canadian Society of Exploration Geophysicists*, v. 6, no. 1, 1969.
- Graul, J. M. and Judson, R. D., The directivity pattern of continuous signals: unpublished paper, 39th Annual Meeting of the Society of Exploration Geophysicists.
- Merritt, R. K., Seismic reflection measurements in the Canadian Arctic Islands: *Proceedings of the 1973 CSEG National Convention*.